Supporting Information

A new mitochondria-targeted fluorescent probe for exogenous and endogenous superoxide anion imaging in living cells and pneumonia tissue

Ya-Xi Ye[a], Jian-Cheng Pan[a], Xin-Yue Chen[a], Li Jiang[c], Qing-Cai Jiao[a,], Hai-Liang Zhu[a,]*, Jun-Zhong Liu[b,]*, Zhong-Chang Wang[a,]*

[a]State Key Laboratory of Pharmaceutical Biotechnology and Institute of Artificial Intelligence Biomedicine, Nanjing University, Nanjing, 210023, PR China; [b]Nanjing Institute for Comprehensive Utilization of Wild Plants, CHINA CO-OP, 211111, Nanjing, China; [c]State Key Laboratory of Desert and Oasis Ecology, Xinjiang Institute of Ecology and Geography, Chinese Academy of Sciences, 830011, Urumqi, China

Contents

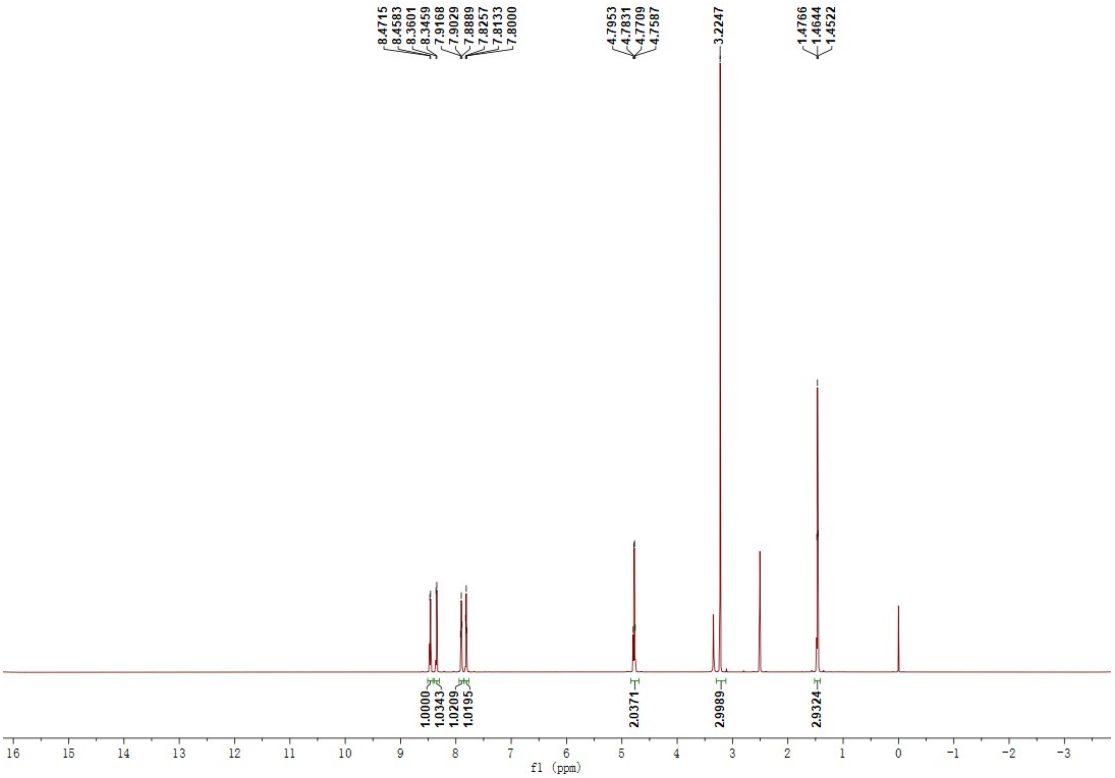

Fig. S1. ^{1}H NMR spectra of **1** (DMSO-d_6).

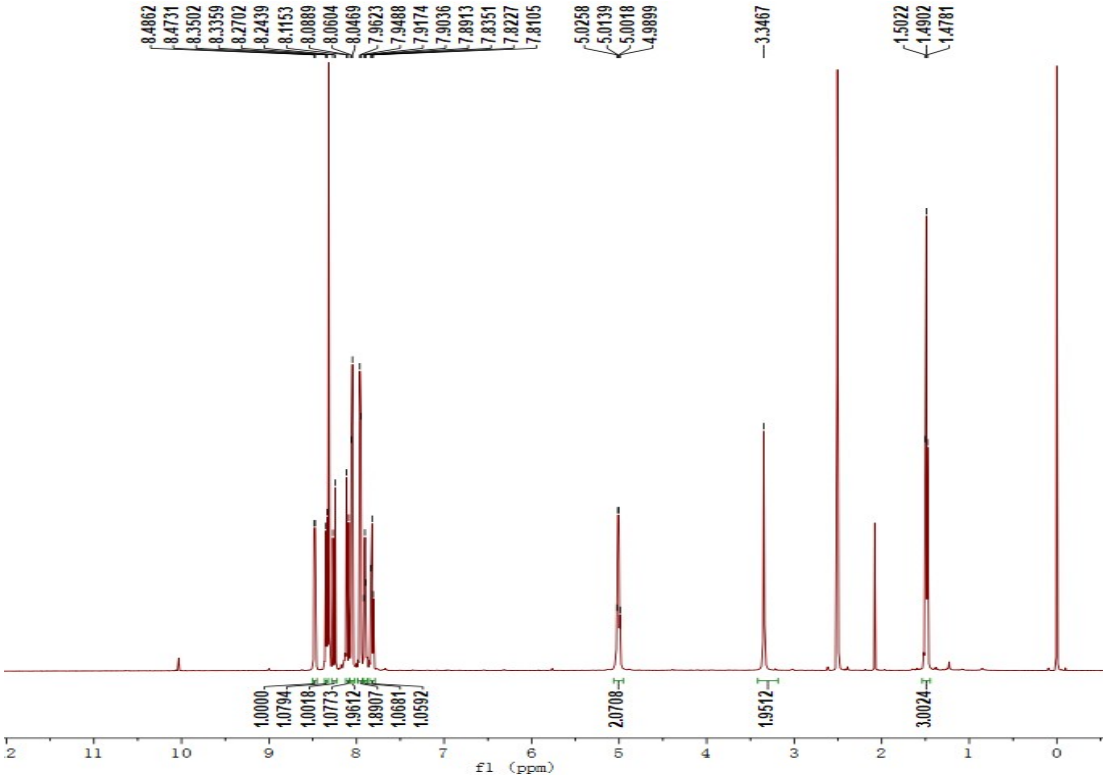

Fig. S2. ^{1}H NMR spectra of **Mito-YX** (DMSO-d_6)

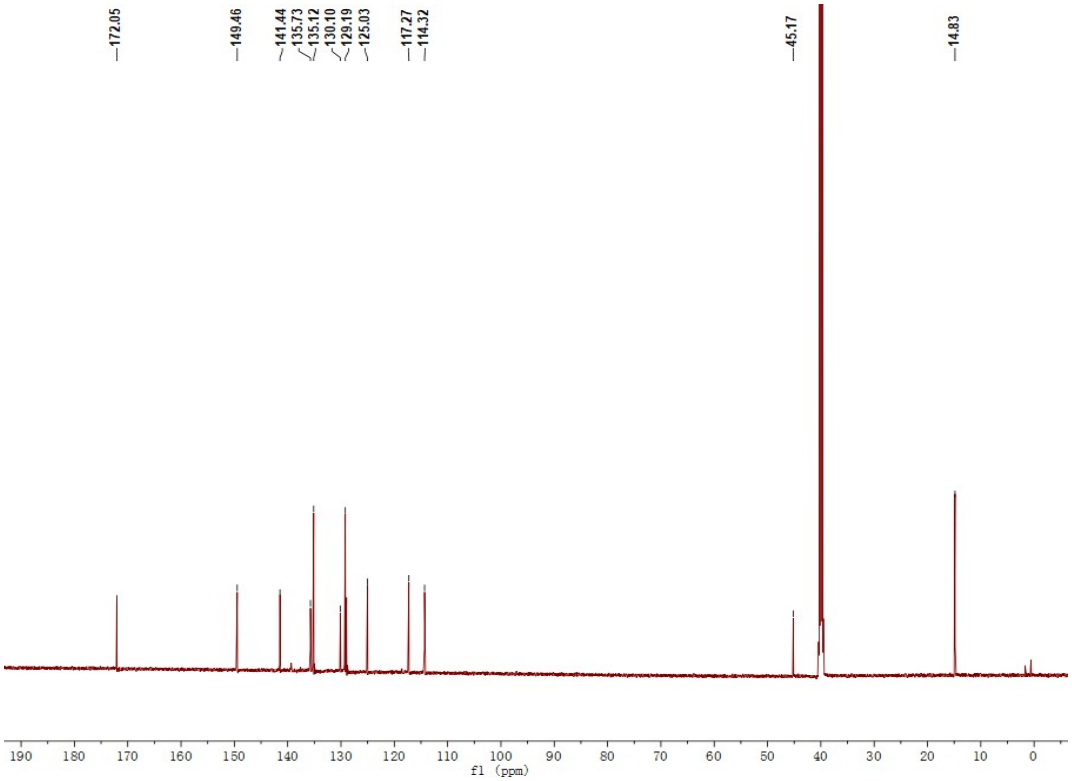

Fig. S3. ^{13}C NMR spectra of **Mito-YX** (DMSO-d_6).

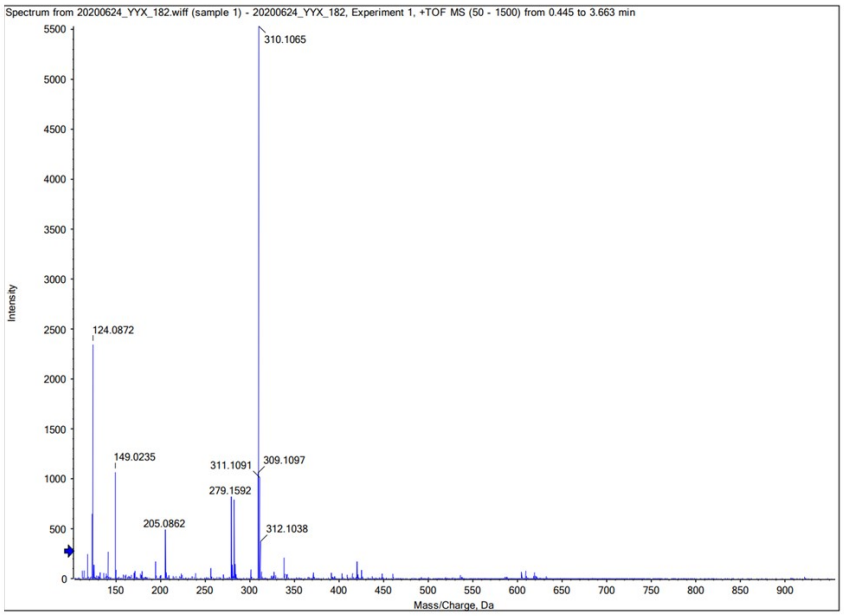

Fig. S4. TOF-MS of **Mito-YX** calculated for $C_{17}H_{17}BNO_2S^+$ $[M]^+$, 311.2; found, 311.1091.

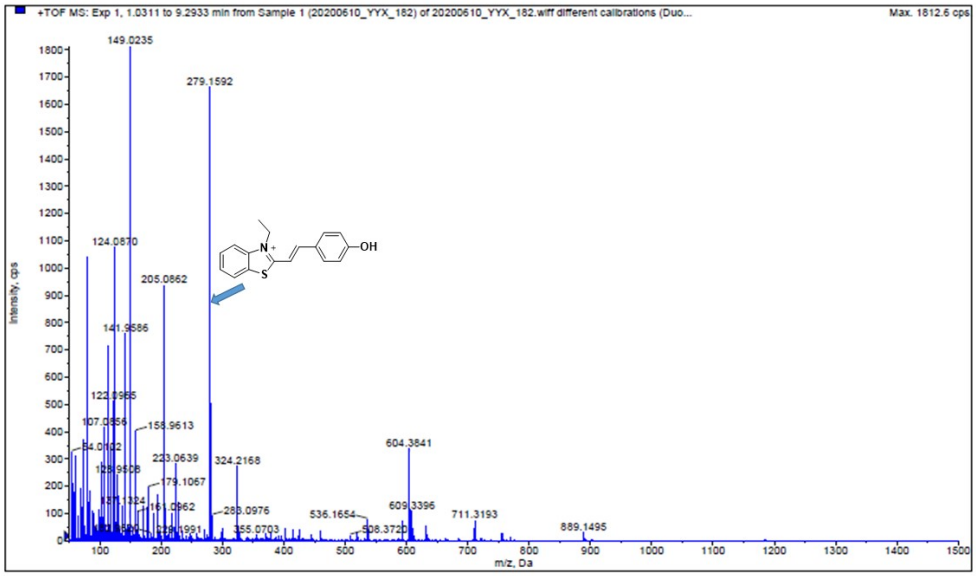

Fig. S5. TOF-MS of the reaction product of **Mito-YX** after treatment with $O_2^{\bullet-}$.

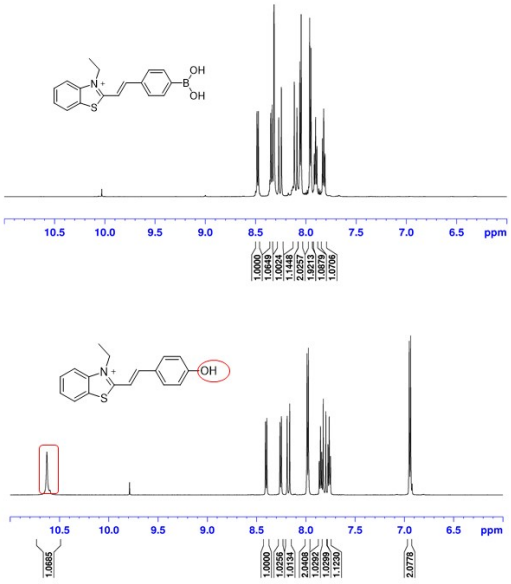

Fig. S6. ^{1}H NMR data of **Mito-YX** and corresponding compounds after reacting with $O_2^{\bullet-}$.

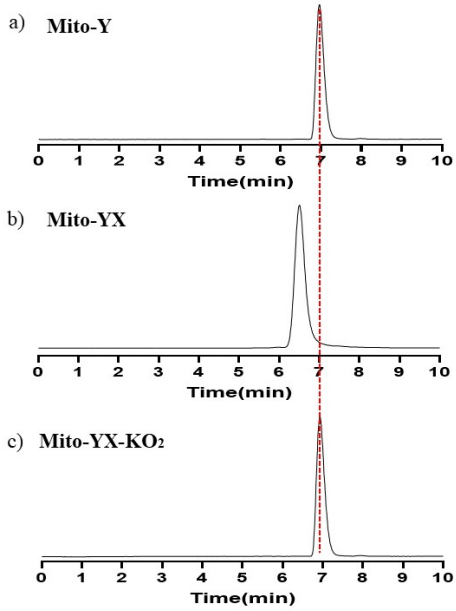

Fig. S7. HPLC chromatogram changes of 10 μM **Mito-Y** (a) and10 μM **Mito-YX** in the absence (b) and presence (c) of 700 μM KO_2.

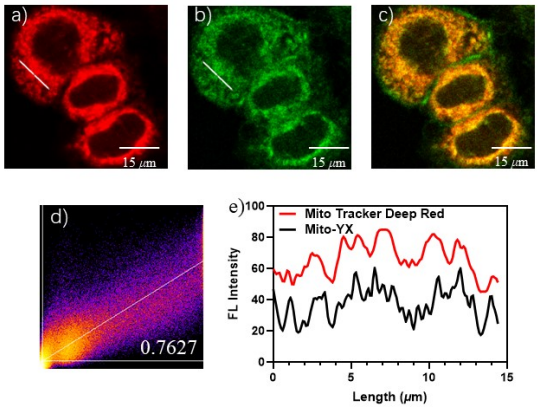

Fig. S8. CLSM images of MCF-7 cells co-cultured with (a) Mito Tracker Deep Red FM (100 nM, red channel); (b) **Mito-YX** (10 μM, green channel, 100 μM KO_2). (c) Overlay image of (a), (b); (d) Intensity correlation plot of Mito Tracker Deep Red FM and **Mito-YX**, R^2 = 0.7627; (F) Intensity profile of the linear ROI across the cell (white line in images panels b–c). green channel: λem = 530-600 nm, λex =488 nm; red channel: λem = 650-670 nm, λex =644 nm. Scale bar: 15 μm.

The Fluorescent quantum yield of **Mito-Y** was studied in 20% ethanol solution using Rhodamine B (Φs=0.89 in ethanol) as a standard. The Fluorescent quantum yields were determined based on the equation:

$$\Phi_u = \left[\left(A_s F_u n^2\right)/\left(A_u F_s n_0^2\right)\right]\Phi_s$$

(Φ_u *and* Φ_s: the fluorescent quantum yield of **Mito-Y** and Rhodamine B, A_u *and* A_s: the absorbance of **Mito-Y** and Rhodamine B respectively, F_u *and* F_s: the integrated fluorescence intensity of **Mito-Y** and Rhodamine B at their excitation wavelength, n presents the refractive index of solvent. The fluorescent quantum yield of **Mito-Y** is 0.23.

Φ_s=0.89，A_s=0.249，F_s= 122297.444，n_0=1.33；A_u=0.131, F_u= 17356.607，n = 1.365; calculated Φ_u = 0.23.

Table.1 The comparison of reported work with this work

Probe	Targeting effect	Ex/Em (nm)	δ	LOD	Time	Application	ref
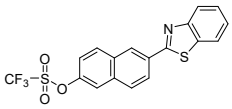	No	λex=365/720 nm; λem=500 nm	/	1 nM	5 min	in buffer, living cells and tissues.	[1]
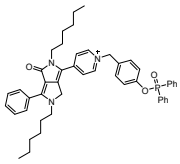	mitochondrion	λ_{ex} = 490 nm; λ_{em}=652/545 nm	/	20.5 nM	3 min	in buffer, living cells, LPS-induced mice	[2]
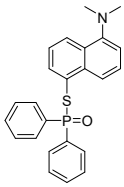	No	λ_{ex}=345/740 nm; λ_{em}=470 nm	/	150 nM	25 min	in buffer, living cells and fresh rat hippocampal tissues	[3]
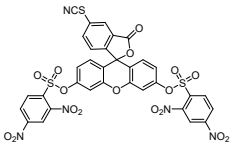	mitochondrion	λ_{ex}= 494 nm, λ_{em}=520 nm	/	0.65 μM	< 5 min	in buffer, living cells	[4]
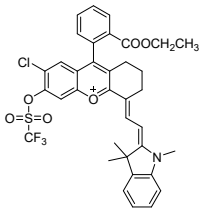	mitochondrion	λ_{ex}= 660 nm, λ_{em}=719 nm	0.55	0.24 μM	/	in buffer, living cells and drug-induced AKI mouse	[5]
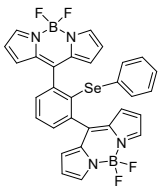	No	λ_{ex}= 505 nm, λ_{em}=526 nm	/	4.42 μM	40 min	in buffer and living cells	[6]
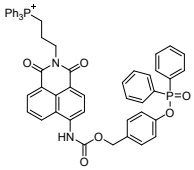	mitochondrion	λ_{ex}= 415 nm, λ_{em}=540/475 nm	/	0.37 μM	132 s	in buffer, living cells and inflammatory Daphnia magna	[7]
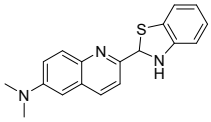	No	λ_{ex}= 430/820 nm, λ_{em}=550 nm	0.19	13 nM	100 s	in buffer, living cells, zebrafish and inflammator	[8]

						y mice	
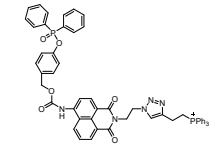	mitochondrion	λ_{ex}= 410 nm, λ_{em}=540/475 nm	EtOH:0.924 DMSO:0.791 PBS:0.497	/	5 min	in buffer, living cells, and inflammatory mice	[9]
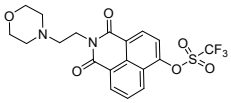	lysosome	λ_{ex}= 450/730 nm, λ_{em}=556 nm	/	0.047 nM	60 min	in buffer, living cells, zebrafish and pneumonia tissue	[10]
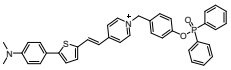	mitochondrion	λ_{ex}= 418nm, λ_{em}=635 nm	/	22.2 nM	20 min	in buffer and living cells	[11]
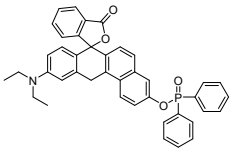	No	λ_{ex}=580/800nm, λ_{em}=638 nm	/	2.09 μM	150 s	in buffer, living cells and diabetic mice	[12]
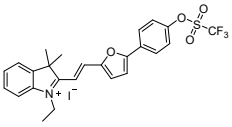	mitochondrion	λ_{ex}=500nm, λ_{em}=645 nm	/	10 nM	/	in buffer and living cells	[13]
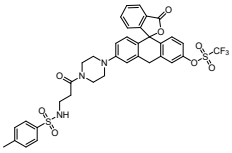	endoplasmic reticulum	λ_{ex}=500/800nm, λ_{em}=558 nm	0.41	0.12 μM	6 min	in buffer, living cells and zebrafish	[14]
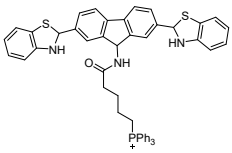	mitochondrion	λ_{ex}=483/800nm, λ_{em}=512 nm	0.1	9.5 nM	/	in buffer, living cells and inflammatory mice	[15]
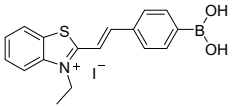	mitochondrion	λ_{ex}=482nm, λ_{em}=565nm	0.23	0.24 nM	4 min	in buffer, living cells and pneumonia tissue	This work

[1] D. Lu, L. Zhou, R. Wang, X.B. Zhang, L. He, J. Zhang, X. Hu, W. Tan, A two-photon fluorescent probe for endogenous superoxide anion radical detection and imaging in living cells and tissues, *Sensor Actuat B-Chem.* 250 (2017) 259-266.

[2] J. Wang, L. Liu, W. Xu, Z. Yang, Y. Yan, X. Xie, Y. Wang, T. Yi, C. Wang, J. Hua, Mitochondria-targeted Ratiometric Fluorescent Probe Based on Diketopyrrolopyrrole for Detecting and Imaging of Endogenous Superoxide Anion in Vitro and in Vivo, *Anal. Chem.* 91 (2019), 5786-5793.
[3] L. Chen, M.K. Cho, D. Wu, H.M. Kim, J. Yoon, Two-Photon Fluorescence Probe for Selective Monitoring of Superoxide in Live Cells and Tissues, *Anal. Chem.* 91 (2019), 14691-14696.
[4] Fang, Si, Yang, Liu, Kelu, Yan, Wenwan, Zhong, A mitochondrion targeting fluorescent probe for imaging of intracellular superoxide radicals, *Chem. Commun.* 51 (2015), 7931-7934.
[5] Y. Lv, D. Cheng, D. Su, M. Chen, B.-C. Yin, L. Yuan, X.-B. Zhang, Visualization of oxidative injury in the mouse kidney using selective superoxide anion fluorescent probes, *Chem. Sci.* 9 (2018) 7606-7613.
[6] A. Ppd, B. An, B. Skm, A. Stm, Phenylselenyl containing turn-on dibodipy probe for selective detection of superoxide in mammalian breast cancer cell line - ScienceDirect, *Sensor Actuat B-Chem.* 281 (2019) 8-13.
[7] Z. Zhang, J. Fan, Y. Zhao, Y. Kang, J. Du, X. Peng, Mitochondria-Accessing Ratiometric Fluorescent Probe for Imaging Endogenous Superoxide Anion in Live Cells and Daphnia magna, *Acs Sensors* 3 (2018) 735-741.
[8] R.Q. Li, Z.Q. Mao, L. Rong, N. Wu, Z.H. Liu, A Two-Photon Fluorescent Probe for Exogenous and Endogenous Superoxide Anion Imaging in vitro and in vivo, *Biosens. Bioelectron.* 87 (2017) 73-80.
[9] Z.A. Ning, H.A. Yun, A. Qt, B. Yw, Z.A. Qiang, H.A. Ping, A mitochondrial targeting two-channel responsive fluorescence probe for imaging the superoxide radical anion in vitro and in vivo, *Talanta* 194 (2019) 79-85.
[10] S. Ma, Y. Ma, Q. Liu, W. Lin, A two-photon fluorescent probe with lysosome targetability for imaging endogenous superoxide anion in living cells, zebrafish and pneumonia tissue, *Sensor Actuat B-Chem.* 332 (2021) 129523.
[11] A. Cx, C. Wxb, A. Zy, A. Sl, W. Yu, A. Jh, A turn-on mitochondria-targeted near-infrared fluorescent probe with a large Stokes shift for detecting and imaging endogenous superoxide anion in cells, *J. Photoch. Photobio. A* 415 (2021), 113304.
[12] W. Song, B. Dong, Y. Lu, Z. Li, W. Lin, Two-photon Fluorescent Sensors for Visual Detection of Abnormal Superoxide Anion in Diabetes Mice, *Sensor Actuat B-Chem.* 332 (2021) 129537.
[13] J.A. Shan, A. Jz, Y.B. Si, A. Xm, A highly responsive, sensitive NIR fluorescent probe for imaging of superoxide anion in mitochondria of oral cancer cells, *Talanta* 222 (2021), 121566.
[14] Y. Lu, R. Wang, Y. Sun, M. Tian, B. Dong, Endoplasmic reticulum-specific fluorescent probe for the two-photon imaging of endogenous superoxide anion ($O_2^{\cdot-}$) in live cells and zebrafishes, *Talanta* 225 (2020) 122020.
[15] L. Ping, Z. Wen, K. Li, L. Xiao, T. Bo, Mitochondria-Targeted Reaction-Based Two-Photon Fluorescent Probe for Imaging of Superoxide Anion in Live Cells and in Vivo, *Anal. Chem.* 85 (2013) 9877-9881.